Analytical and Numerical Studies of the Beta-Effect in Tropical Cyclone Motion. Part I: Zero Mean Flow

JOHNNY C. L. CHAN* AND R. T. WILLIAMS

Department of Meteorology, Naval Postgraduate School, Monterey, CA 93943

(Manuscript received 30 August 1985, in final form 10 November 1986)

ABSTRACT

The β-effect on tropical cyclone motion is studied using an analytical as well as a numerical model in a nondivergent barotropic framework. The analytical model and the linear version of the numerical model give essentially the same result: the linear β-effect causes a westward stretching of the model vortex but no significant movement of the vortex center. An east–west asymmetry in the meridional wind field is also created. It is the inclusion of the nonlinear term that produces the northwestward movement of the vortex previously found by other investigators (e.g., Kitade, 1981). This northwestward movement increases with both the maximum wind speed and the radius of maximum wind in a constant-shape vortex. A wind maximum is also found to the northeast of the vortex, which appears to be consistent with the observational findings of Shea and Gray. This asymmetry plays an important role in the vortex motion.

1. Introduction

The study of the effect of the earth's rotation on the movement of a tropical cyclone dates back to the work of Rossby (1939, 1948). Since then, a number of theoretical and numerical studies have been conducted to examine this effect (see the review in Chan, 1982). Rossby suggested that the larger Coriolis force on the poleward side of a symmetric cyclonic vortex would produce a net force which would cause the cyclone to move poleward. On the other hand, Adem and Lezama (1960) and later Anthes and Hoke (1975) and others proposed that differential advection of the earth's vorticity to the west and east of the cyclone would cause it to move initially westward. A secondary circulation (in the horizontal) is then set up which advects the vortex northward (Holland, 1983). As a result, the cyclone tends to move towards the northwest. This has become known as the β-effect.

However, some questions regarding the physical processes associated with this main effect remain. For example, what is the mechanism that sets up the secondary circulation? How do the linear and nonlinear processes contribute to the movement of the cyclone? Is the β-effect independent of the intensity of the vortex? This study attempts to address these questions by solving the nondivergent barotropic vorticity equation. The numerical results of DeMaria (1983, 1985) suggest that cyclone movement is rather insensitive to the intensity of the cyclone. However, his results were obtained with the cyclone embedded in a basic flow. Exclusion of any mean flow in this study will allow reexamination of the sensitivity of the cyclone movement to its intensity due to the beta effect. In Part II, the interaction between the vortex flow and different mean flows will be analyzed.

A simple analytical solution of the nondivergent barotropic vorticity equation is first sought to determine the effect of linear processes on the vortex movement. This effect is also demonstrated with a finite-difference numerical model, which indicates that the finite difference resolution is adequate to resolve the physical processes on the vortex scale. The numerical model is then used to study the nonlinear terms which cannot be easily included in the analytical model. Implications of these results on our understanding of the effect of the Coriolis parameter on both the motion and structure of the vortex will also be discussed.

2. Analytical model

a. Formulation

The nondivergent barotropic model used in this study can be formulated in terms of the conservation of absolute vorticity. The governing equation is

$$\frac{\partial \zeta}{\partial t} + \mathbf{V}_\psi \cdot \nabla(\zeta + f) = 0, \tag{2.1}$$

where ζ is the vertical component of the relative vorticity, $\mathbf{V}_\psi$ the nondivergent wind vector, and f the Coriolis parameter. A streamfunction ψ can be defined such that

$$\nabla^2 \psi = \zeta. \tag{2.2}$$

* Present affiliation: Royal Observatory, Hong Kong.

The linearized version of (2.1) with no mean flow on an equatorial beta plane can then be written

$$\frac{\partial}{\partial t}\left(\frac{\partial^2\psi}{\partial x^2}+\frac{\partial^2\psi}{\partial y^2}\right)+\beta\frac{\partial\psi}{\partial x}=0, \tag{2.3}$$

where β is the latitudinal variation of the Coriolis parameter.

Assuming periodic boundary conditions in both the x and y directions, the Fourier transform of (2.3) gives

$$\frac{\partial\Psi}{\partial t}-\frac{ik\beta}{(k^2+l^2)}\Psi=0, \tag{2.4}$$

where

$$\Psi(k,l,t)=\int_0^{2\pi}\int_0^{2\pi}\psi(x,y,t)e^{i(kx+ly)}dxdy, \tag{2.5}$$

and k, l are the wavenumbers in the x and y directions, respectively. If the function Ψ is separable in time and the temporal part is oscillatory, then it can be written as

$$\Psi(k,l,t)=A(k,l)e^{-i\omega t}. \tag{2.6}$$

Substituting (2.6) into (2.4) yields

$$A(k,l)=\Psi(k,l,0) \tag{2.7}$$

and

$$\omega=-\frac{k\beta}{k^2+l^2}. \tag{2.8}$$

The streamfunction at any time t is then given by the inverse transform of $\Psi(k, l, t)$ as

$$\psi(x,y,t)=\frac{1}{2\pi}\sum_k\sum_l A(k,l)e^{-i(kx+ly+\omega t)}. \tag{2.9}$$

Given the initial conditions $\psi(x, y, 0)$, we can then solve for $\psi(x, y, t)$ using (2.5) and (2.7)–(2.9). Note that since the wavenumber l in the y-direction only appears as l^2 in (2.8), the solution will be symmetric about the x-axis.

The cyclonic vortex used in this part of the study has a tangential wind $V(r)$ profile of

$$V(r)=V_m\left(\frac{r}{r_m}\right)\exp\left\{\frac{1}{b}\left[1-\left(\frac{r}{r_m}\right)^b\right]\right\}, \tag{2.10}$$

where r is the radius, V_m the value of $V(r)$ at the radius of maximum wind r_m and b is a factor that determines the shape of the vortex. Examples of this profile can be found in Fig. 1 for different values of V_m. The corresponding vorticity (ζ) profile is given by

$$\zeta(r)=\frac{2V_m}{r_m}\left[1-\frac{1}{2}\left(\frac{r}{r_m}\right)^b\right]\exp\left\{\frac{1}{b}\left[1-\left(\frac{r}{r_m}\right)^b\right]\right\}. \tag{2.11}$$

One method to initialize the model just described is to solve for ψ from (2.2) and (2.11). However, a simpler method is to use the $\zeta(r)$ profile directly by first noting the equality

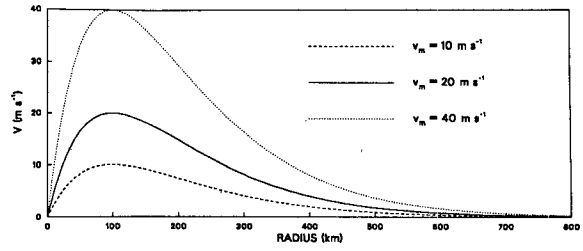

FIG. 1. Tangential wind profiles as defined in (2.10) for different values of V_m.

$$\int_0^{2\pi}\int_0^{2\pi}[\nabla^2\psi(x,y,0)]e^{i(kx+ly)}dxdy$$
$$=-(k^2+l^2)\int_0^{2\pi}\int_0^{2\pi}\psi(x,y,0)e^{i(kx+ly)}dxdy$$

so that

$$A(k,l)=-\frac{1}{(k^2+l^2)}\int_0^{2\pi}\int_0^{2\pi}\zeta(x,y,0)e^{i(kx+ly)}dxdy. \tag{2.12}$$

The streamfunction at any time t is then obtained by solving (2.9), with the spectral amplitude $A(k, l)$ of the initial conditions given by (2.12). In the following, solutions of (2.9) using a grid size of 20 km and 101 grid points in both the x and y directions will be presented. Beta is evaluated at 10° latitude.

b. Results

The streamfunction fields at selected times for a vortex given by (2.10) with V_m = 40 m s^{-1}, r_m = 100 km and b = 1.0 are shown in Fig. 2. The vortex is seen to elongate westward with time as a result of the dispersive effects of Rossby waves. The dispersion relation given by (2.8) implies that longer waves have larger westward phase speeds than shorter waves. Since the waves representing the outer circulation have lower wavenumbers than those representing the inner circulation, the outer part of the vortex propagates westward faster than the inner part, which results in a stretching of the vortex westward. Such a dispersion of linear Rossby waves has also been studied for ocean vortices (e.g., Flierl, 1977; McWilliams and Flierl, 1979; Mied and Lindemann, 1979).

The time variations of the relative vorticity fields are similar to those of the streamfunction and therefore will not be shown. However, it must be noted that in solving for ζ from (2.2) and (2.9), the amplitudes of the spectral coefficients $A(k, l)$ are reduced by a factor $(k^2 + l^2)$ so that the westward propagation of shorter waves (representing the inner circulation) will be further decreased. As a result, even though the ψ and ζ fields are initially concentric, the β-effect produces an intersection of the two fields, as illustrated in Fig. 3.

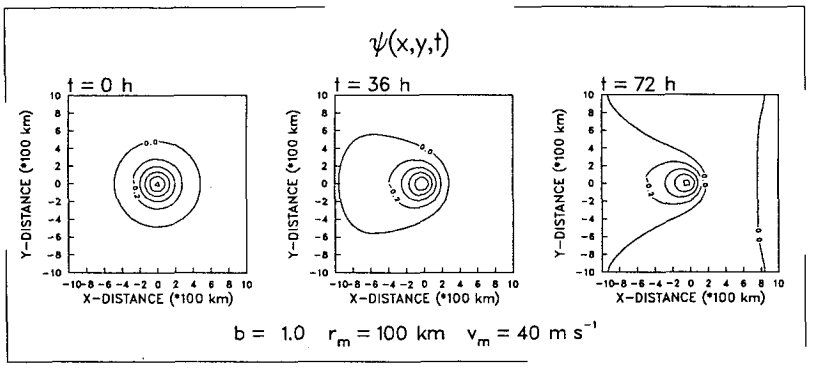

FIG. 2. Streamfunction fields (ψ) at 0, 36 and 72 h for the analytical model using the vortex profile in (2.10) with $V_m = 40$ m s^{-1}, $r_m = 100$ km and $b = 1.0$. The contour interval is 0.2×10^6 m^2 s^{-1}.

Notice that the intersection of the ψ and ζ isolines occurs near the center of the vortex where not much movement of the vorticity maximum occurs. Since the streamfunction represents the flow field, such an intersection between the two fields becomes important when the effect of relative vorticity advection (not considered in this formulation) is included.

The asymmetry in the ψ field (Fig. 2) also implies an asymmetry in the wind fields. Since the streamfunction is symmetric about the x-axis, the wind asymmetry is only in the meridional (v) component (Fig. 4) and results in a wind maximum to the east of the vortex. Note also that the speed differential between the east and west sides of the vortex increases with time.

The large east–west wind asymmetry may be explained as follows. Advection of the earth vorticity produces an increase (decrease) in relative cyclonic vorticity to the west (east) of the vortex. Since the governing equation (2.3) implicitly assumes an instantaneous adjustment of the winds, these changes in relative vorticity will increase the southerly flow near, and northerly flow at distances both east and west of, the vortex center. This southerly flow was first identified by Anthes and Hoke (1975) and termed the "secondary circulation" by Holland (1983). Because the winds are initially northerly to the west and southerly to the east of the vortex, this secondary circulation will produce an east–west asymmetry in the v-component. As only linear effects are included in the model, this asymmetry cannot be removed through self-advective (nonlinear) processes. At the same time, the increase in southerly flow further decreases the relative vorticity near and to the east of center through the advection of the earth's vorticity. The asymmetry in the wind field therefore increases with time.

If the rate of decay of the tangential wind with radius is decreased (that is, the value of b is reduced in Eq. 2.10), the center of the vortex (where the stream func-

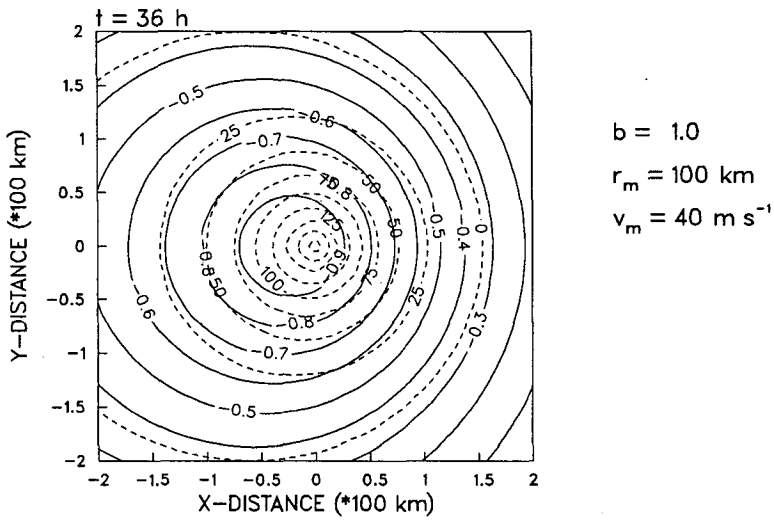

FIG. 3. As in Fig. 2 except for the streamfunction (solid, 10^6 m s^{-1}) and relative vorticity (dashed, 10^{-5} s^{-1}) fields at 36 h.

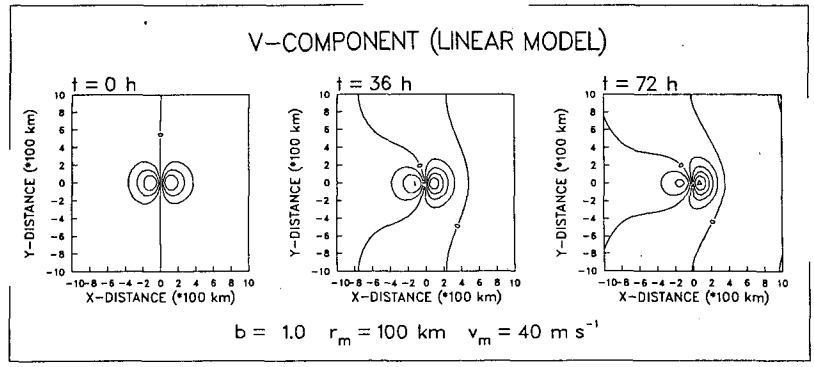

FIG. 4. Meridional (v) wind component at 0, 36 and 72 h derived from the solutions in Fig. 2. The contour interval is 10 m s^{-1}.

tion is a minimum) is found to have a slightly larger westward displacement (not shown). This results from the longer waves associated with a larger vortex having a larger amplitude so that the westward phase speed is enhanced. For the same reason, a constant-shape vortex with a larger radius of maximum wind (r_m in Eq. 2.10) will move westward faster than one with a smaller r_m. However, varying the magnitude of the maximum wind (V_m) does not have an effect on the vortex movement. An increase in the value of V_m simply increases the amplitudes of the spectral coefficients $A(k, l)$ by the same amount for all wavenumbers (see Eq. 2.12). This results in the values of $\psi(x, y, t)$ obtained by solving (2.9) being multiplied by a larger factor but the location of the relative minimum in the streamfunction remains unchanged.

To summarize, the linear β-effect elongates a symmetric vortex westward with very little displacement of the center of the vortex (as given by the maximum of relative vorticity or minimum in streamfunction). The wind field also becomes highly asymmetric in the east–west direction with stronger (weaker) winds to the east (west).

3. The numerical model

a. Formulation

The nondivergent barotropic model developed by Tupaz (1977) to study barotropic instabilities associated with an easterly jet (Tupaz et al., 1978) is utilized. The governing equation with no mean flow can be written as

$$\frac{\partial}{\partial t}\nabla^2\psi = -J(\psi, \nabla^2\psi) - \beta\frac{\partial\psi}{\partial x}, \tag{3.1}$$

where the symbols are as in section 2. The Jacobian $J(\psi, \nabla^2\psi)$ represents the nonlinear effect that is excluded in section 2. The domain is an east–west channel with cyclic boundary conditions in the zonal direction. That is,

$$\psi = 0 \quad \text{at} \quad y = \pm D, \tag{3.2}$$

where the meridional domain is defined by

$$-D \leqslant y \leqslant D.$$

Eq. (3.1) is solved using the leapfrog time-differencing scheme. The Jacobian is evaluated using the finite difference form developed by Arakawa (1966). At the north–south boundaries, the values of $\nabla^2\psi$ are extrapolated from the first interior points. The direct method described by Sweet (1973) is used to solve for $\partial\psi/\partial t$ in (3.1) and to derive the initial streamfunction field from the vorticity profile defined in (2.11).

The linear [with $J(\psi, \nabla^2\psi)$ set to zero] solutions to (3.1) are found to be very similar to those from the analytical model. The similarity of the results from the two models provides an indication that the truncation errors in the numerical solutions are small.

b. Results

The nonlinear solutions to (3.1) for the same vortex used in section 2 are shown in Fig. 5. Contrary to the linear solution (Fig. 2), the inner part of the vortex remains rather symmetric. At the same time, the outer part of the vortex maintains a westward stretching as a result of the linear β-effect. The vortex center is now displaced to the northwest. An acceleration in the movement of the vortex can also be identified from its track (Fig. 6), with its translation speed increasing from 0.8 m s^{-1} in the first 12 h to 2.8 m s^{-1} by 60 h. Notice also a slight oscillation in the vortex track.

Such a northwestward displacement and acceleration of the vortex as well as the oscillation in the track are consistent with results obtained by other researchers (e.g., Kitade, 1981). This movement can be explained by considering the east–west asymmetry induced by the β-effect discussed in section 2. Since the nonlinear term (advection of vortex vorticity) is now included, the crossing of the ψ and ζ isolines shown in Fig. 3 implies an advection of the vortex vorticity by the

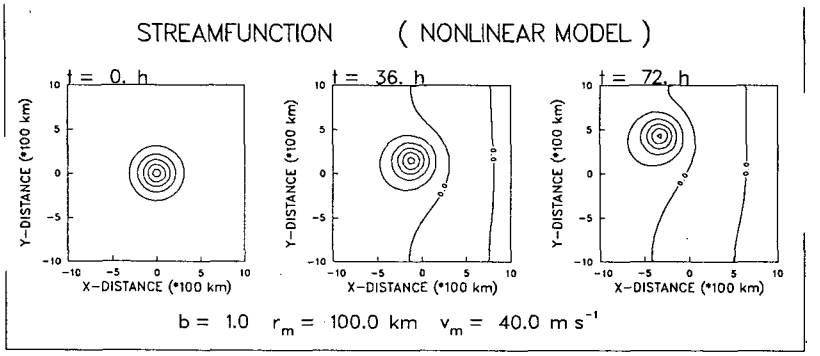

FIG. 5. As in Fig. 2 except for the nonlinear numerical simulations. The contour interval is 0.1×10^6 m^2 s^{-1}.

asymmetric flow represented by the streamfunction ψ. This advection leads to an increase of vorticity to the north of the vortex and a decrease to the south. These changes in vorticity depend on the crossing angle between the ψ and ζ isolines. Near the vortex center, the crossing angle and the speed are large and thus a strong advective (nonlinear) effect results. In the outer region, the two fields do not intersect significantly so that this part of the vortex continues its westward elongation while the inner region moves northward. Consequently, the asymmetry in the streamfunction field is no longer east–west but rather along a southwest–northeast direction (Fig. 5).

The physical explanation given here of the northwestward vortex displacement due to the β-effect is somewhat different from that schematically portrayed by Holland (1983). According to Holland (1983), the vortex first moves west due to the beta effect. Then the vorticity changes lead to a secondary circulation which is directed to the north over the vortex center, which combined with the beta effect causes the vortex to move to the northwest. In the present study the early northward motion is caused by relative vorticity advection which results from the Rossby wave distortion of the vortex. At a later stage when the wind asymmetry is developed (Fig. 7), the asymmetry has associated with it a flow component across the center in the direction of movement. This is generally consistent with Holland's view of the role of the secondary circulation.

Because of the orientation of the streamfunction asymmetry (Fig. 5), the maximum wind speed is now to the northeast of the vortex (Fig. 7). Notice also an oscillation of the 40 m s^{-1} isotach around the northeastern quadrant of the vortex. The maximum wind increases from 41.6 m s^{-1} at 12 h to 43.5 m s^{-1} at 48 h. If the translation speed is subtracted, a residual asymmetry still remains. Therefore, this wind asymmetry cannot be explained simply by the translation of the vortex. Adjustments of the wind field to the increase in relative vorticity to the northwest of the vortex (due to the nonlinear effect) tends to produce a wind maximum in this region but the (linear) β-effect induces a wind maximum to the east of the vortex. A combination of these two effects therefore causes a continuous adjustment between the ψ and ζ fields, which leads to the wind asymmetry and the associated oscillations. The oscillation in the vortex track can also be explained in a similar manner as the vortex tries to move along a "constant phase" line which balances the linear and the nonlinear effects. Part of this oscillation may be due to difficulty in finding the center between grid points, but the increase in speed is well defined.

The existence of an asymmetry in the tangential winds in tropical cyclones after the motion of the cyclone is removed has been observed by several researchers (e.g., Jordan, et al., 1960; Shea and Gray, 1973; George and Gray, 1976). The asymmetry is usually to the right of the cyclone (facing downstream along the direction of cyclone motion). Most tropical cyclones (in the Northern Hemisphere) move westward or northwestward. Thus, this asymmetry would be in the northeast quadrant, which is consistent with the numerical result presented here. Therefore, the combination of the beta (linear) and the nonlinear effects may offer an explanation of such an observed asymmetry.

To summarize, it is the combination of the linear and nonlinear effects that leads to a northwestward displacement of the vortex. The continuous distortion of the streamfunction and relative vorticity fields by the β-effect causes an adjustment between these two fields to occur when nonlinear (horizontal advection of vortex vorticity) effects are included. A modification of either effect will therefore lead to a change in the vortex movement, as will be seen in section 4.

4. Sensitivity tests with vortex strength and scale

In this Section, results are presented from integrations with different values of r_m and V_m in the initial vortex (2.10), but with the original value $b = 1$. The following grid sizes are used for each value of the radius of maximum wind: $r_m = 50$ km, $\Delta x = \Delta y = 10$ km; $r_m = 100$ km, $\Delta x = \Delta y = 20$ km; $r_m = 200$ km and $\Delta x = \Delta y = 40$ km. All experiments use a domain size

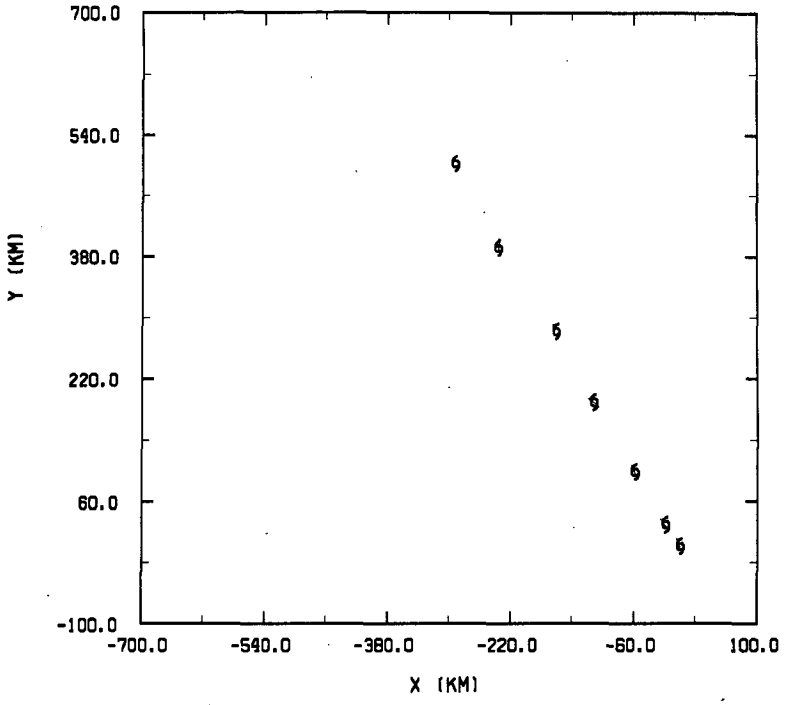

FIG. 6. The 0–72 h track of the vortex with r_m = 100 km, V_m = 40 m s^{-1}. The symbols along the track are 12 h apart.

of 201 × 201 which insures that the boundaries do not affect even the fastest moving vortex over 72 hours. In each experiment the form of the vortex trajectory is similar to that shown in Fig. 6 for r_m = 100 km and V_m = 40 m s^{-1}. All results presented in this section are averages from t = 48 hours to t = 72 hours. The directions of motion for the various experiments are given in Table 1. They have a monotonic variation from 315° to 335°. For a fixed r_m, the angle increases with increasing V_m, and the angle decreases for increasing r_m when V_m is fixed. The curves in Fig. 8 give the speed of movement as a function of V_m for each of the three values of r_m. The curves imply a linear behavior as a function of V_m for $V_m \leq 20$ m s^{-1}, but note that the curves do not extrapolate to the origin as $V_m \to 0$. This may be related to the vastly different structure type in the highly distorted Rossby wave solution ($V_m = 0$) as compared with the nearly circular solution when V_m is small, but not zero. This strongly suggests that one cannot get the proper solution by expanding about the linear solution. Figure 9 contains movement curves as a function of r_m for three values of V_m. In this case, the portions of the curves which satisfy $r_m \leq 100$ km do appear to extrapolate to zero as $r_m \to 0$. Figure 10

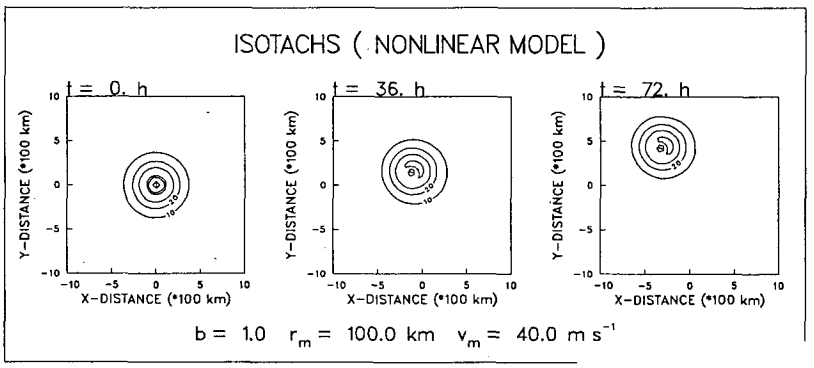

FIG. 7. Isotachs derived from the nonlinear numerical simulation given in Fig. 5. The contour interval is 10 m s^{-1}.

TABLE 1. Directions of movement averaged from 48 to 72 h for each experiment.

V_m (m s^{-1})	r_m (km)		
	50	100	200
2.5		321.1°	
5.0		321.7°	
10.0	330.3°	324.8°	314.4°
20.0	332.2°	328.9°	318.6°
40.0	333.9°	329.3°	325.9°
80.0		334.1°	

contains contours of the speed of movement as a function of r_m and V_m. The curves are roughly hyperbolic, which would be expected since the curves in Figs. 8 and 9 have approximately linear variations.

These results show that the speed of movement of the vortex increases with V_m and r_m, although the direction changes only slowly. If the "angular momentum", $r_m V_m$, is held constant in Fig. 10, it can be seen that the speed of movement is nearly constant (since the isolines in Fig. 10 are nearly hyperbolas). This suggests that a tropical cyclone track would be unaffected by changes in intensity provided that $r_m V_m$ were conserved. Holland (1984) states that "no track changes accompany oscillations in central pressure or maximum winds in hurricanes". However, it is not known whether or not $r_m V_m$ is conserved in these cases. Our solutions (see especially Fig. 9) indicate that the winds in the outer region have more influence on the vortex motion than winds closer to the center. In fact DeMaria (results presented by Holland, 1984) showed that increasing the wind in the inner part of the vortex (r < 100 km) had no effect on vortex motion while changes in the outer region had a direct effect. DeMaria (1983, 1985) found similar results in a model which included horizontal wind shear as well as the beta effect.

5. Discussion and conclusion

The results from this study can be summarized as follows. The linear β-effect, though incapable of significantly displacing the central core of the vortex, provides a necessary environment for vortex movement. It creates an east–west asymmetry in the meridional wind field which then interacts with the vortex vorticity when nonlinear effects are included. Advection of the vortex vorticity then gives rise to a northwestward displacement of the vortex. This nonlinear process depends on the strength of the meridional wind field created by the linear effect and the relative vorticity gradient within the vortex. An increase in the tangential winds at all radii causes an increase in the northwestward movement although the linear β-effect remains unchanged. Increasing the size of the vortex with the shape held fixed enhances the meridional flow through the linear dispersion of Rossby waves and leads to a larger northwestward displacement. The solutions show that the speed of movement is nearly constant for vortices which have the same characteristic "angular momentum" $r_m V_m$. The results of this paper agree with the previous conclusion (Holland, 1983, 1984 and DeMaria, 1983, 1985) that the vortex motion is insensitive to the wind structure in the inner region.

Another consequence of the combination of the (linear) β-effect and the nonlinear effect is the creation of a wind maximum to the northeast of the vortex. It

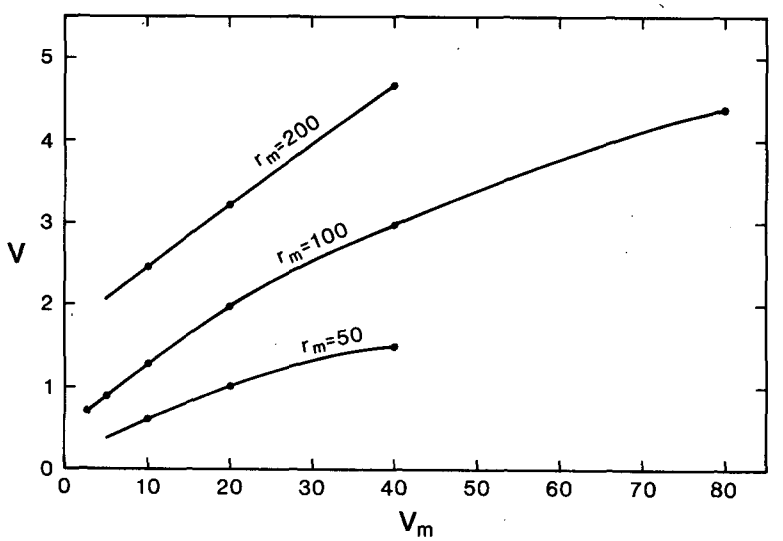

FIG. 8. The speed of movement V (m s^{-1}) as a function of V_m (m s^{-1}) for three values of r_m (km).

appears that this asymmetry plays an important role in the vortex motion. Such an across-the-vortex wind asymmetry has been found from aircraft observations of hurricanes (Shea and Gray, 1973). The β-effect may therefore offer an explanation of this observed asymmetry.

From the fluid dynamical point of view, this study shows how dispersion (linear) and vorticity advection (nonlinear) effects can combine to move the vorticity center even though neither process can significantly move the vortex by itself. It is very important to obtain a more complete understanding of this process.

No mean flow is included in these experiments in order to isolate the β-effect. As is discussed in section 4, incorporation of a basic flow significantly complicates the problem. DeMaria (1985) has pointed out the importance of the vorticity gradient associated with the basic flow. The linear advection of the vortex by a spatially nonuniform basic flow will also modify the vortex movement. In addition, the dispersion of Rossby waves can occur with this basic flow. Nonlinear interactions between the vortex circulation and the basic flow can also alter the movement of the vortex. All these effects will be presented in Part II of this study.

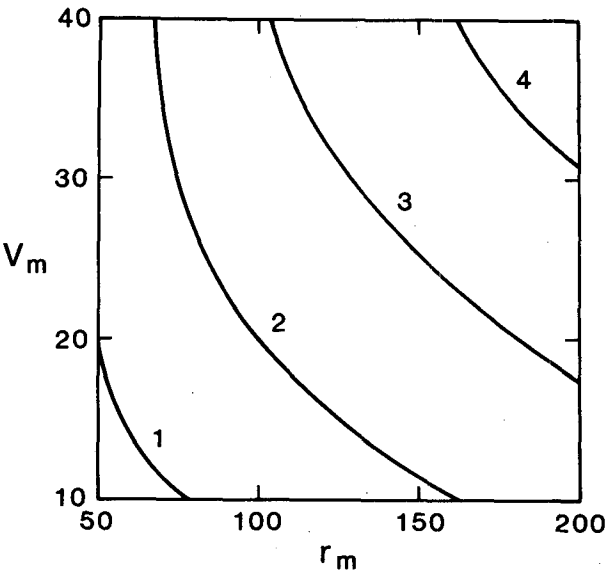

FIG. 10. Isolines of the speed of movement V (m s^{-1}) as functions of V_m (m s^{-1}) and r_m (km).

Acknowledgments. The authors would like to thank Mr. M. Fiorino for performing all of the numerical integrations which are presented in section 4, and especially for finding a critical error in the original computer code. The authors would also like to thank Professor R. L. Elsberry, Dr. Greg Holland and Dr. Mark DeMaria for helpful comments on the manuscript. Mrs. Penny Jones carefully typed the manuscript and Mr. Mike McDermet drafted some of the figures. This research was supported by the National Science Foundation Global Atmospheric Research Program under Grant ATM 8315175 and the Naval Air Systems Command through the Naval Environmental Prediction Research Facility.

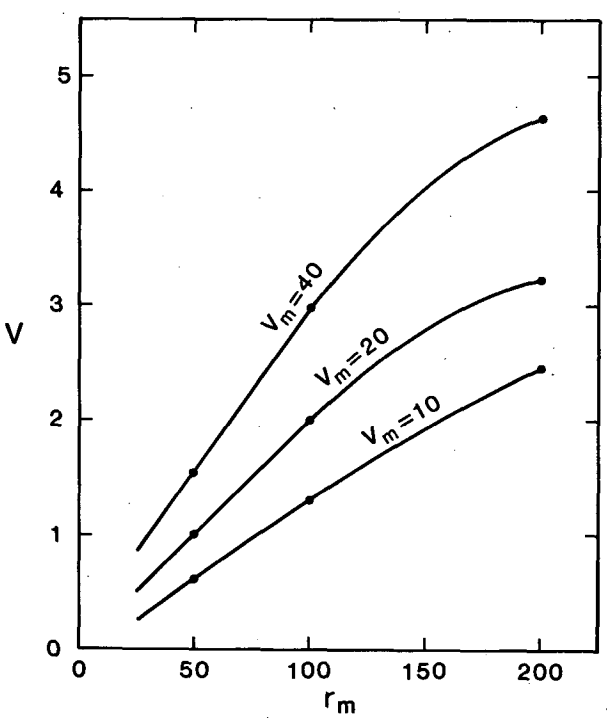

FIG. 9. The speed of movement V (m s^{-1}) as a function of r_m (km) for three values of V_m (m s^{-1}).

REFERENCES

Adem, J., and P. Lezama, 1960: On the motion of a cyclone embedded in a uniform flow. *Tellus,* **12,** 255–258.

Anthes, R. A., 1982: Tropical Cyclones: their evolution, structure and effects. *Meteor. Monographs,* Vol. 19, No. 41, Amer. Meteor. Soc., 208 pp.

——, and J. A. Hoke, 1975: The effect of horizontal divergence and the latitudinal variation of the Coriolis parameter on the drift of a model hurricane. *Mon. Wea. Rev.,* **103,** 757–763.

Arakawa, A., 1966: Computational design for long-term numerical integration of the equations of atmospheric motion. *J. Comput. Physics,* **1,** 119–143.

Chan, J. C.-L., 1982: On the physical processes responsible for tropical cyclone motion. *Atmos. Sci. Paper* No. 358, Department of Atmospheric Science, Colorado State University, Fort Collins, CO, 200 pp.

DeMaria, M., 1983: Experiments with a spectral tropical cyclone model. *Atmos. Sci. Paper* No. 371, Department of Atmospheric Science, Colorado State University, Fort Collins, CO, 224 pp.

——, 1985: Tropical cyclone motion in a nondivergent barotropic model. *Mon. Wea. Rev.,* **113,** 1199–1210.

Flierl, G. R., 1977: The application of linear quasi-geostrophic dynamics to Gulf Stream rings. *J. Phys. Oceanogr.,* **7,** 365–379.

George, J. E., and W. M. Gray, 1976: Tropical cyclone motion and

surrounding parameter relationships. *J. Appl. Meteor.*, **15,** 1252–1264.

Holland, G. J., 1983: Tropical cyclone motion: Environmental interaction plus a beta effect. *J. Atmos. Sci.*, **40,** 328–342.

——, 1984: Tropical cyclone motion: A comparison of theory and observation. *J. Atmos. Sci.*, **41,** 68–75.

Jordan, C. L., D. A. Hurt and C. A. Lowry, 1960: On the structure of Hurricane Daisy of 27 August 1958. *J. Meteor.*, **17,** 337–348.

Kitade, T., 1981: A numerical study of the vortex motion with barotropic models. *J. Meteor. Soc. Japan,* **59,** 801–807.

McWilliams, J. C., and G. R. Flierl, 1979: On the evolution of isolated, nonlinear vortices. *J. Phys. Oceanogr.*, **9,** 1155–1182.

Mied, R. P., and G. J. Lindemann, 1979: The propagation and evolution of cyclonic Gulf Stream rings. *J. Phys. Oceanogr.*, **9,** 1183–1206.

Rossby, C. G., 1939: Relation between variations in the intensity of the zonal circulation of the atmosphere and the displacements of the semi-permanent centers of action. *J. Marine Res.*, **2,** 38–55.

——, 1948: On displacements and intensity changes of atmospheric vortices. *J. Marine Res.*, **7,** 157–187.

Shea, D. J., and W. M. Gray, 1973: The hurricane's innner-core region. I: symmetric and asymmetric structure. *J. Atmos. Sci.*, **30,** 1544–1564.

Sweet, R. A., 1973: A generalized cyclic reduction algorithm. *SIAM J. Num. Anal.*, **10,** 506–520.

Tupaz, J. B., 1977: A numerical study of barotropic instability of a zonally varying easterly jet. Ph.D. Thesis, Naval Postgraduate School, Monterey, CA, 107 pp.

——, R. T. Williams and C.-P. Chang, 1978: A numerical study of barotropic instability in a zonally varying easterly jet. *J. Atmos. Sci.*, **35,** 1265–1280.